SUPPLEMENTAL INFORMATION

Methods for B1+ and Sice Profile correction.

Our approach to B_1^+ and slice profile correction was devised to accommodate the large range of B_1^+ variation we observed across the abdomen (0.5 – 1.5, in terms of relative flip angle). B_1^+ values determined by a separate B_1^+ mapping scan were used to select the appropriate dictionary for T_1 and T_2 matching. We implemented slice profile correction by approximating the slice profile for all excitations in the pulse train by a scaled version of the slice profile for the maximum achieved FA (nominal FA multiplied by B_1^+). This approximation meant that the series of FA experienced by each isochromat (i) across the slice were scaled versions of each other, where the scale is determined by isochromat location. Thus, a slice profile and B_1^+ corrected dictionary could be assembled by the weighted sum of individual simulations for each isochromat:

$$I_{corrected}(T_1, T_2, B_1^+) = \sum_{i=1}^{N} W_{sp}(rFA_i(B_1^+)) \times I(T_1, T_2, rFA_i) \ , \quad (1)$$

where weights and simulations corresponding to each isochromat are $W_{sp}(rFA_i(B_1^+))$ and $I(T_1, T_2, rFA_i)$, respectively. We generated a dictionary using an extended phase graph simulation for all combinations of T_1, T_2 and rFA_i (between 0.02 and 1.5, in 0.02 increments). To be clear, the simplifying approximation described above meant that each simulation was for the series of FA where the nominal FA series (Figure 1 A) was multiplied by rFA_i. We calculated slice profiles (M_{xy}) for the maximum achieved flip angle for each B_1^+ value (FA_{max} = 78° multiplied by B_1^+) for the implemented excitation pulses (Hanning-windowed sinc, duration = 2 ms, time bandwidth product = 4) in a range four times the nominal slice width and for 1001 isochromats using rftools [59]. W_{sp} were determined by taking the fraction of discrete positions (r_i) across each simulated slice profile when $(abs(M_{xy}(r_i))/78°$ was between $(rFA_i + rFA_{i-1})/2$ and $(rFA_i + rFA_{i+1})/2$. See Figure 1 B for an example slice profile.

B_1^+ maps were smoothed and interpolated to match the resolution of the MRF acquisition and to mitigate motion corruption of the in vivo B_1^+ maps (Figure 1 C-F). Motion and different k-space acquisition trajectories meant that the B_1^+ maps were not perfectly aligned to the MRF images. Since B_1^+ variations have low spatial frequency, maps were smoothed by fitting with a 6th-order polynomial, and then interpolated to have the same resolution and FOV as the raw MRF images. The relative flip angle estimate for each voxel was used as prior information for dictionary matching.

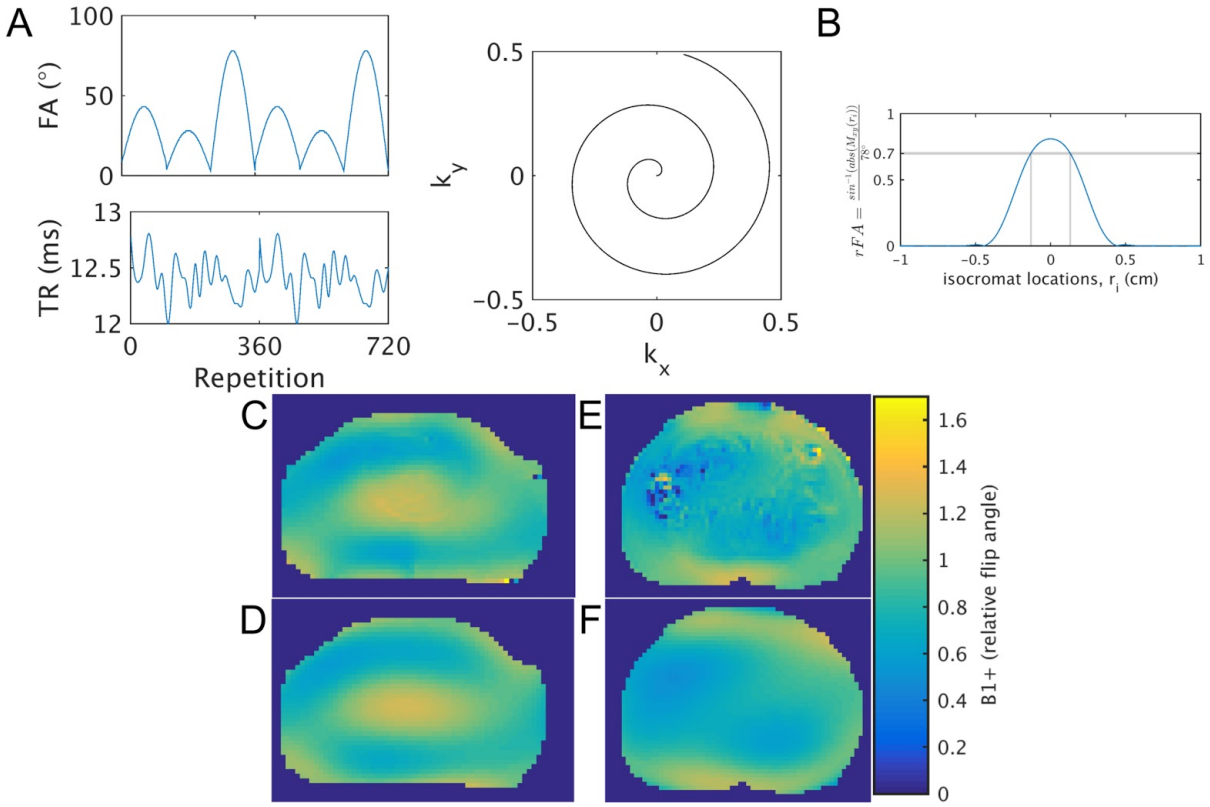

Figure S1. Methods. The sinusoid variation in flip angles (FA) and the perlin noise pattern variation in repetition times (TR) used in the sequence and one interleave of the continuous density spiral readout (A). Slice profile for an example region (B) where the B_1^+ inhomogeneity is such that the spins achieve only 80% of the nominal FA for each excitation pulse. Thus the maximum FA in the series is 0.8*78 = 62.4. To determine, for example, the weight in Equation 1 (W_{sp}) for $I(T_1,T_2,0.7)$, the fraction of isochromats with 0.69<rFA<0.71 (horizontal gray rectangle) is 0.012 (12/1001). Post-processing of the B_1^+ map for use in MRF dictionary matching demonstrated on a phantom modeling a 22-week GA fetus. B_1^+ map is acquired (C), and then smoothed by fitting 6th-order polynomial (D). In vivo B_1^+ maps sometimes have motion artifacts from fetal motion or swirling amniotic fluid (E) that are minimized by smoothing (F).

Table S1. Reference and MRF-determined relaxation times for the NIST phantom T_1- and T_2-arrays. Values presented as median (interquartile range) of relaxation time across hand-drawn ROIs.

T1 array				
Array number	T1 GT [ms]	T1 MRF [ms]	T2 GT [ms]	T2 MRF [ms]
1	1989	2020 (75)	1465	1550 (200)
2	1454	1460 (110)	1076	1150 (215)
3	984	1070 (60)	718	742 (36)
4	706	750 (60)	510	562 (48)
5	497	540 (80)	360	358 (57)
6	352	390 (40)	256	235 (30)
7	247	270 (80)	181	198 (55)
8	175	200 (55)	127	145 (48)
9	126	130 (40)	90	84 (32)
10	89	100 (20)	64	73 (20)
11	63	60 (0)	46	37 (8)
12	45	40 (15)	32	32 (22)
13	31	40 (0)	22	34 (8)
14	22	20 (20)	16	18 (27)
T2 array				
Array number	T1 GT [ms]	T1 MRF [ms]	T2 GT [ms]	T2 MRF [ms]
1	2480	2460 (80)	581	544 (72)
2	2173	2260 (60)	404	394 (36)
3	1907	1960 (105)	278	275 (34)
4	1604	1680 (80)	191	200 (15)
5	1332	1350 (80)	133	117 (20)
6	1044	1100 (120)	97	80 (22)
7	802	840 (130)	64	65 (21)
8	609	630 (100)	46	47 (16)
9	458	480 (60)	32	27 (12)
10	336	340 (60)	22	22 (10)
11	244	260 (45)	16	16 (8)
12	177	180 (20)	11	14 (8)
13	127	160 (20)	8	10 (1)
14	91	120 (20)	6	10 (5)

Figure S2. Visualization of the effects of slice profile and B1+ corrections individually on T_2 and T_1 values for the 22-week anthropomorphic phantom. The symbol marks the median parameter value and the error bars show IQR of the voxels within the hand-drawn ROI. The ROIs are represented by color and shown in the inset of Fig 2E: maternal abdomen (blue), placenta (red), fetal body (green), and fetal brain (magenta). The measurement types are represented by symbols: reference or ground truth (x), uncorrected MRF (triangle), B1+ correction only (square), slice-profile correction only (star), and B_1^+ and slice profile corrected MRF (circle). Note that in the placenta ROI (red) the two corrections individually yield the same median value, but the IQR is narrower for the SPC-T_1 (25 ms) and B_1+-T_2 (30 ms).

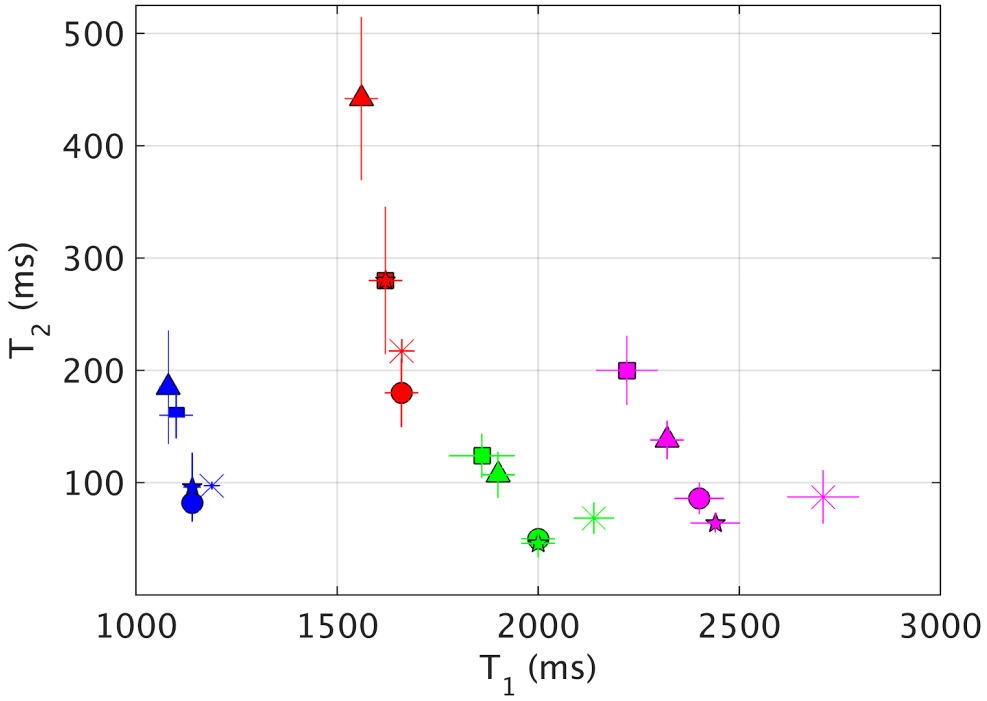

Figure S3. Motion and no motion. Example T_1 (A, C) and T_2 (B, D) parameter maps during hyperoxia without motion (A, B) and with motion (C, D) for GA 35w2d. Motion causes a depression in T_2 estimates (arrows) and a blurring in T_1 most clearly seen in the fetal brain (oval). Acquisition was in the transverse plane while subject was in the left lateral position.

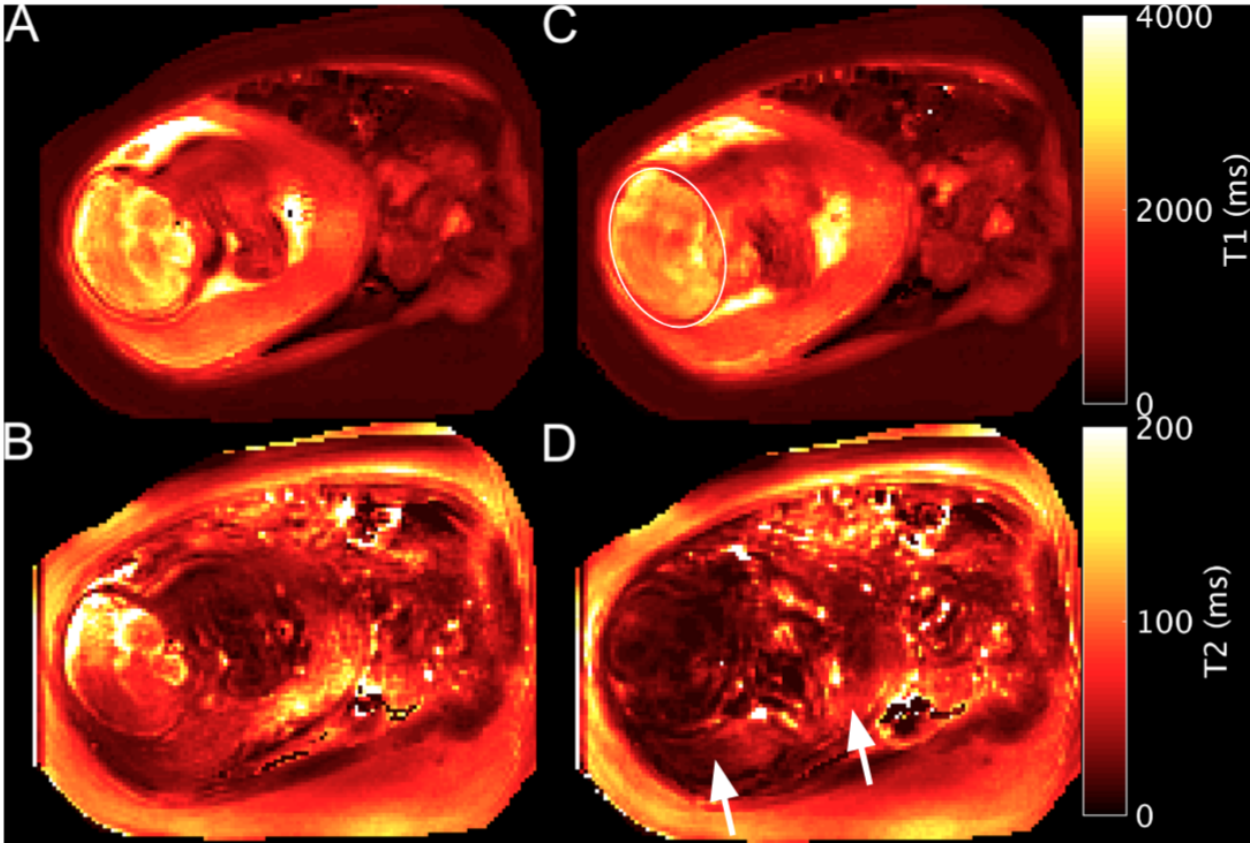

Table S2. Summary of all MRF measurements. Each cell is mean(median(ROI)) +/- std(median(ROI)). "--" indicates that there was only one motion-free measurement for this subject. "na" indicates that this region and state was not acquired. "motion" indicates that this measurement was motion corrupted (after subject 10 we collected three MRF acquisitions to mitigate motion corruption).

		Placenta ROI			
		air		O_2	
Subject number	GA [wk+day]	T_1 [ms]	T_2 [ms]	T_1 [ms]	T_2 [ms]
1	27+1	2000 ± 0	42 ± 0	na	na
2	36+5	1500 ± 0	32 ± 0	na	na
3	34+4	1580 ± 0	52 ± 0	1800 ± 0	52 ± 0
4	34+2	motion	motion	motion	motion
5	34+0	motion	motion	motion	motion
6	32+3	1700 ± 0	50 ± 0	1620 ± 0	40 ± 0
7	34+3	1780 ± 0	82 ± 0	motion	motion
8	28+5	1880 ± --*	64 ± --	motion	motion
9	29+2	motion	motion	1840 ± --	60 ± --
10	34+5	2000 ± --	54 ± --	2040 ± --	48 ± --
11	35+3	1840 ± 80	62 ± 7	1825 ± 35	76 ± 11
12	35+6	1780 ± 75	60 ± 2	1753 ± 12	77 ± 4
13	29+6	1867 ± 31	70 ± 7	1810 ± 71	78 ± 6
14	34+4	1910 ± 12	72 ± 2	1880 ± 0	76 ± 0
15	35+3	2020 ± 0	34 ± 0	1880 ± 0	48 ± 0
16	34+6	1777 ± 31	83 ± 4	1807 ± 85	69 ± 4
17	27+1	1835 ± 21	53 ± 1	motion	motion
18	32+1	1553 ± 12	47 ± 5	1580 ± --	56 ± --
19	34+6	1820 ± --	48 ± --	1840 ± --	60 ± --
20	34+0	1990 ± 32	86 ± 4	1987 ± 23	87 ± 2
21	30+4	1953 ± 27	58 ± 5	1950 ± 0	52 ± 0
22	29+6	1760 ± 72	72 ± 4	1820 ± --	62 ± --
23	29+2	1900 ± 35	71 ± 8	1900 ± --	64 ± --
24	32+2	1680 ± 0	54 ± 0	1650 ± 42	49 ± 1
25	33+5	1900 ± 208	53 ± 6	1970 ± 12	54 ± 14
26	25+6	1980 ± 57	76 ± 0	na	na

27	24+2	1880 ± --	94 ± --	1680 ± 198	79 ± 21
28	29+4	1625 ± 52	58 ± 5	1595 ± 29	60 ± 2
29	36+2	1820 ± --	54 ± --	na	na
30	29+4	1960 ± 0	43 ± 2	1970 ± 42	48 ± 0
31	31+4	1813 ± 10	48 ± 2	1907 ± 27	71 ± 1

Figure S4. Histograms of voxelwise T_1 and T_2 estimates for the placental ROIs for all subjects with motion-free acquisitions. Color represents GA.

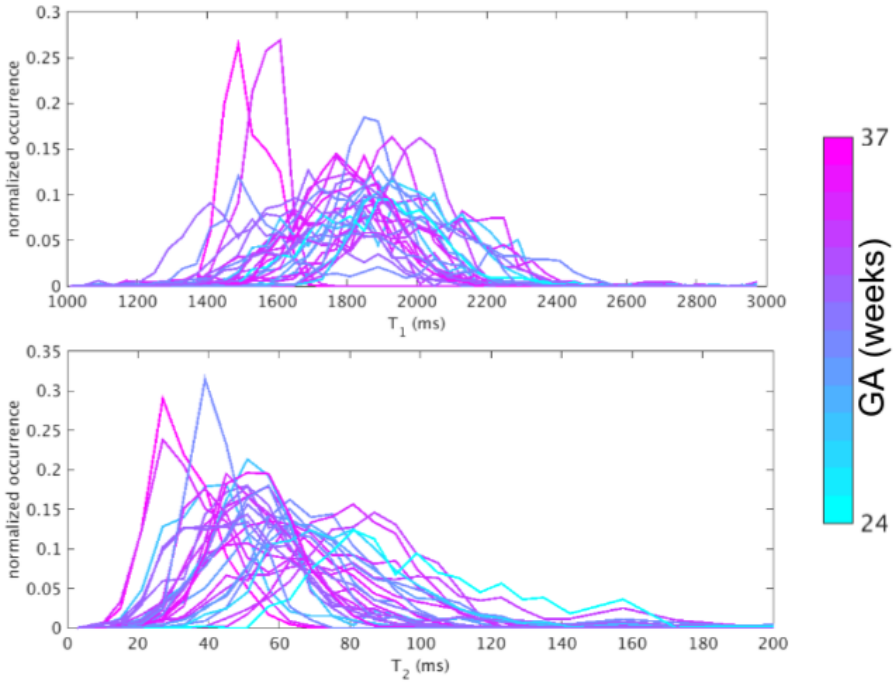

Table S3. Mean+/-standard deviation multiple MRF measurements from different parallel slices. Each measurement was summarized by, as elsewhere, the median of the hand-drawn ROI of the placenta. Significant differences between slice measurements (P<0.05) is indicated by *.

Placenta		MRF		
Subject/Slice	slice	T1	T2	N_meas
11	1	1880+/-20	59+/-8	3
11	2	1780+/-113	66+/-6	2
12	1	1680+/-0*	58+/-0	2
12	2	1790+/-14*	61+/-1	2
20	1	1980+/--35	86+/--3	3
20	2	2020+/--0	85+/--7	2

Detection of motion from "fully-sampled" mixed contrast MRF images presented as movies:

subj11_still_MID02903_slwin30_meas1to720.avi

subj11_motion_MID02904_slwin30_meas1to720.avi

Each movie consists of 691 consecutive images reconstructed via the sliding window method (34).